



73rd Conference of the Italian Thermal Machines Engineering Association (ATI 2018),
12–14 September 2018, Pisa, Italy

Control strategies for a powertrain with hydromechanical transmission

Antonio Rossetti^a Alarico Macor^{b,†}

^aNational Research Council – Construction Technologies Institute, Padova, Corso Stati Uniti, 4, 35127 Padova, Italy

^bDepartment of Engineering and Management, University of Padova, Stradella S. Nicola, 3, 36100 Vicenza, Italy

Abstract

This paper deals with the management of an engine equipped with a continuous hydro-mechanical transmission.

The traditional minimum fuel consumption control strategy requires the control system to keep the engine along the minimum fuel consumption line. However, this strategy may not be the best one, since the performance of the powertrain depends on both engine efficiency and transmission efficiency.

Therefore, a methodology was developed in order to extend the minimum fuel consumption control strategy for the engine to the engine-transmission set, that is, to the whole powertrain.

To achieve this goal, the case of an urban bus equipped with a dual-stage hydromechanical transmission was studied. The vehicle's powertrain model was first used to derive the family of minimum consumption curves for the powertrain; subsequently to simulate the behavior of the vehicle. The comparison between the minimum consumption criterion for the engine and the minimum consumption criterion for the powertrain shows a slight advantage of the latter.

© 2018 The Authors. Published by Elsevier Ltd.

This is an open access article under the CC BY-NC-ND license (<https://creativecommons.org/licenses/by-nc-nd/4.0/>)

Selection and peer-review under responsibility of the scientific committee of the 73rd Conference of the Italian Thermal Machines Engineering Association (ATI 2018).

Keywords: Optimal management; Fuel consumption; Power-Split transmission

1. Introduction

Fuel consumption and emission reduction are the main drivers in the improvement of agricultural and heavy duty mobile machinery. The scientific research identified three main strategies to achieve these goals: the electrical [1] or hydraulic hybridization [2, 3], the improvement and the optimal management of the hydraulic powered tools [4, 5], and the adoption of advanced transmissions, such as the hydromechanical transmission [6,7].

In recent years, this transmission has spread in the field of high power agricultural machines, thanks to its good driving comfort. However, its efficiency is slightly lower than the efficiency of manual and powershift transmissions [6, 7]. Therefore, this transmission has been subject to many studies dealing with the design [6 - 9] and the optimization of both components and layout [10 - 12].

In some applications, such as in the public transport sector, the hydromechanical transmission can take advantage of two features: the absence of the torque converter, which in a powershift transmission produces high losses during vehicle starting; and the

* Corresponding author. Tel.: +39 0444 998729; fax: +39 0444 998888.

E-mail address: alarico.macor@unipd.it

Nomenclature

M	vehicle mass [kg]	τ	transmission velocity ratio [-]
P	power [kW]	ω	rotational speed [rad s ⁻¹] or [rpm]
r_w	wheel radius [m]	<u>Subscript</u>	
s	pilot control signal [-]	CVT	Continuously Variable Transmission
T	torque [Nm]	ICE	Internal Combustion Engine
v	vehicle speed [km h ⁻¹]	w	Wheel
η	efficiency [-]	opt	Optimum

possibility to separately manage the engine speed from the vehicle speed [13]. The engine can therefore be managed following the minimum consumption curve or minimum emission curves of the engine [14].

For vehicles equipped with CVT and for hybrid vehicles, the engine control strategies have been divided into two groups: rule-based strategies and optimization-based strategies [15, 16]. In the first group, the rules are designed based on heuristic considerations, human experience and mathematical models, without a priori knowledge of the driving cycle [17, 18]. In the second group, the control strategies are identified by the minimization of the fuel consumption along a predetermined driving cycle [19–21].

However, the engine management following the minimum specific fuel consumption may not be the best one for the vehicle as the performance of the powertrain depends on both functional conditions of the engine and of the transmission. In fact, the efficiency of the powertrain is the product of engine efficiency and transmission efficiency; the latter, however, depends on parameters other than those on which the performance of the engine depends. Therefore, in the engine map should exist a curve of minimum consumption for the entire powertrain distinguished from that of minimum consumption for the engine alone.

In this paper this problem has been faced with the aim of providing some management recommendations for a future application on heavy duty vehicles. The minimum specific fuel consumption line for the powertrain will be identified in the engine map, in analogy to what is usually done for the engine alone. In this way, no complexity has been added to the powertrain management system, but only different minimum lines in the control system. The proposed strategy can be classified as a rule based strategy.

The problem will be investigated studying the powertrain behavior of a 12 m class urban bus, consisting of a diesel engine and a Dual Stage hydromechanical transmission. The powertrain will be modeled in the Amesim environment based on the functional data provided by the manufacturers.

The vehicle model will be used first to derive the minimum fuel consumption lines for the complete powertrain, then to simulate the operation of the vehicle on various road routes. In order to evaluate the benefits of the new control strategy, the optimal management of the entire powertrain will be compared to the optimal management of the engine alone.

2. Control Strategies

The CVT transmission allows the vehicle speed to be separated from the engine speed as the transmission ratio can be adjusted to match the required vehicle speed with the desired engine speed. Nevertheless, this feature is subject to some constraints, given both by the engine and the transmission. In fact, the working point on the engine map must meet the required power on the wheels and, at the same time, must satisfy the minimum and maximum ratios achievable by the CVT transmission:

$$P_{ICE}\eta_{CVT} = P_w \quad (1)$$

$$\omega_{ICE}\tau_{CVT} = \frac{v_w}{r_w} \quad \text{with } \tau_{CVT} \in [\tau_{CVT}^{\min} \dots \tau_{CVT}^{\max}] \quad (2)$$

Then, the presence of a free variable generates the conditions for an optimization criterion of the system management. This criterion can be purely energetic or contemplate figures of merit that include other desirable behaviors, such as noise reduction or pollutant emission control.

The use of the minimum consumption line as a criterion for the choice of engine speed is a very common practice [14]. The line can be defined with the following optimization problem:

for a given output condition P_{ICE} find $\omega_{ICE\ opt}$, which minimizes $1 - \eta_{ICE}$, where:

$$\eta_{ICE} = \eta_{ICE}(\omega_{ICE}, P_{ICE}) \quad (3)$$

under the constraints of Eq. 1-2 and:

$$\omega_{ICE\ opt} \in [\omega_{ICE}^{\min} \dots \omega_{ICE}^{\max}]_{P_{ICE}} \quad (4)$$

The result is a generally continuous curve in the coordinates of the engine map. Assuming as objective the maximization of the efficiency of the whole system, it is necessary to consider both the engine efficiency and the transmission efficiency. While the

former is univocally defined once the working point in the engine map has been identified, the latter is a function of the transmission ratio and the power processed by the transmission. The optimization problem can therefore be formulated as:

for a given output condition ω_w, P_w find $\omega_{ICE\ opt}$, which minimizes $1 - \eta_{ICE} \eta_{CVT}$, where:

$$\eta_{ICE} = \eta_{ICE}(\omega_{ICE}, P_{ICE}) \quad (5)$$

$$\eta_{CVT} = \eta_{CVT}(\tau_{CVT}, P_w) \quad (6)$$

under the constraints of Eq. 1-2 and:

$$\omega_{ICE\ opt} \in \left[\omega_{ICE}^{\min} \dots \omega_{ICE}^{\max} \right]_{P_{ICE}=P_w/\eta_{CVT}} \quad (7)$$

Once the ICE efficiency map (eq.s 3 and 5) and the CVT efficiency (eq. 6) are given, the optimization can be easily solved by using iteratively standard 1-D optimizer and different initializations in order to avoid the risk of local optimum. In the present work Nelder-Mead Simplex Method was used.

By iterating the optimization for different transmission output conditions ω_w, P_w , the optimal locus, $\omega_{ICE\ opt}, v_w, P_w$ can be identified. It can be represented, in the coordinates of the engine map ω_{ICE}, M_{ICE} , as a set of curves parameterized by the vehicle speed v_w .

3. Numerical model

The mechanic and hydraulic elements of the vehicle, as well as the whole control system, were modelled and simulated by using LMS Imagin.Lab AMESim commercial software [22]. The following section will provide some information on the engine model and the control system. Detailed information on the loss models used for the hydraulic and mechanical elements of the transmission can be found in [13]

3.1. Reference vehicle

The reference vehicle is a 12 m urban bus equipped with a 180 kW supercharged - 4 cylinder - Euro 4 diesel engine; its main data are summarized in Table 1.

Table 1. Main characteristics of the reference vehicle.

Model		IVECO-IRISBUS: Cityclass
Wheel drive		Rear
Mass	M	12000 kg
Length		12 [m]
Maximum speed	V_{max}	Limited to 68 km/h

3.2. The hydromechanical transmission

The Dual Stage hydromechanical transmission is used in the reference vehicle (Figure 1). It is a well-known layout derived from the simpler input-coupled transmission substituting the epicyclical gear with an advanced one having two outlets [9, 23]. The efficiency curve of the transmission shows two distinct maxima, at points where the whole power is transmitted through the mechanical transmission branch (Full Mechanical Point, FMP) [9]; this feature guarantees better performance with respect to the input-coupled transmissions, which, instead, admit only one FMP. Figure 1 shows the main components of the transmission: the engine, the variable hydraulic element, the four-shaft planetary train (PGT), the rear axle gear, and the clutches CI and CII for the synchronous gear change.

The variable hydraulic element is a standard hydrostatic transmission, equipped with relief valves, boost pump, counter pressure and flushing valves (not shown in Figure 1). The transmission has been sized to fulfil the acceleration and power requirements of a test case by applying the classical sizing schemes [9, 23]. Its main characteristics are reported in Table 2.

The transmission was equipped with a lock-up clutch (C_0) to disengage the engine, in order to avoid transmission losses during idle time.

The transmission efficiency is shown in the following Figures 5b, 6b, 7b for three different vehicle speeds and in the whole transmission power range.

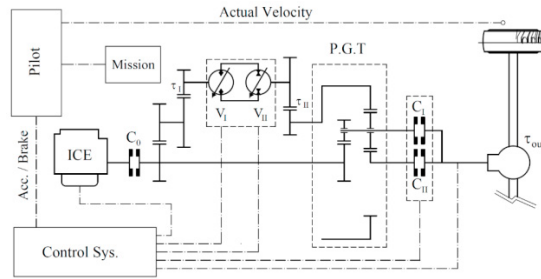


Fig. 1: Power-Split transmission layout.

Table 2. Main data of the hydromechanical transmission

-Unit I		-Unit II	
Gear Ratio τ_I	0.58	Gear Ratio τ_{II}	0.58
Gear Ratio Efficiency	0.98	Gear Ratio Efficiency	0.98
Maximum Displacement	125 cc	Maximum Displacement	125 cc
-Complex Planetary Gear		-Rear Axle Gear Ratio	
Ring Tooth Number	90	Overall Ratio	10.13
First Sun Tooth Number	45	Differential Gear Ratio	4.00
Second Sun Tooth Number	30	Planetary Reducer	2.53
Efficiency	94	Overall Efficiency	0.960

3.3. Engine model

A 180 kW supercharged - 4 cylinder - Euro 4 diesel engine was chosen; its map was derived scaling the map of a 115 kW - 2 l automotive diesel engine (Figure 2).

The engine was modelled as an ideal torque source. The values of the torque and the fuel consumption were expressed as a function of the engine speed and the throttle position. In order to take into account the dynamic effects, the engine inertia and a first order lag in the acquisition of the accelerator signal were included in the model (Figure 3).

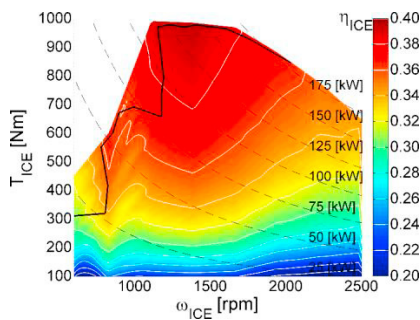


Fig. 2. Map of the ICE.

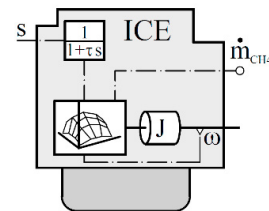


Fig. 3. Dynamic model of the ICE.

3.4. The loads

The vehicle loads, i.e. the aerodynamic friction force F_a , and the rolling friction force F_r , were modelled according to $F_a = 0.5 c_d v^2 A_f$ and $F_r = k_r M \cdot g$. Typical values of the 12 m class bus for the drag coefficient, the frontal area, and rolling resistance coefficient were respectively assumed: $c_d = 1.18$, $A_f = 7 \text{ m}^2$, $k_r = 0.008$.

The vehicle was considered as a translating point having mass M , and no complex dynamic was applied during the simulations. No slope resistance was considered because the test cycles are intended to be undertaken on a flat road.

3.5. The powertrain control system

The scheme of the control system of the powertrain is shown in Figure 4.

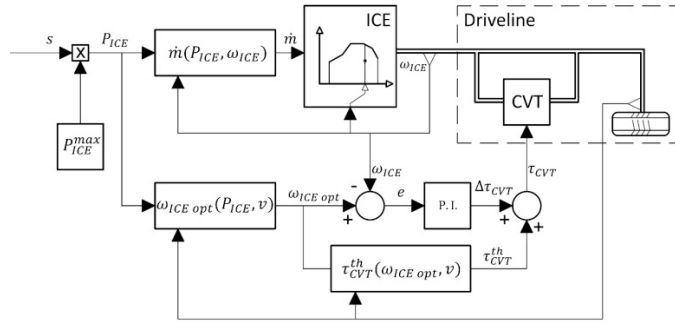


Fig. 4. Control system layout.

The input of the system is given by the position of the accelerator, expressed as a ratio between the power requested by the pilot and the maximum power delivered by the engine: in dimensionless coordinates $s = 0 \div 1$. From this signal and from the knowledge of the current engine speed, the required fuel flow is calculated, thus obtaining control over the power actually supplied by the engine.

The control on the engine speed is assigned to the CVT transmission, whose transmission ratio is governed by a feed forward system corrected by a PI controller, both powered by the optimal speed of the engine, which is estimated on the basis of the current vehicle speed and power requested by the pilot.

4. Results

4.1. Best efficiency line maps

The transmission was numerically characterized by sequentially varying $\omega_w, P_w, \omega_{ICE}$ within their ranges; its efficiency was also mapped. The points considered are shown in Table 3, where the values are shown in terms of vehicle speed, for easier reading.

Table 3. Operating points used for the transmission characterization.

Parameter	min	max	step	Unit
$v = \omega_w r_w$	5	70	5	km/h
P_w	5	90	5	% P_{ICE}^{max}
ω_{ICE}	500	2500	2	rpm

With the characterization results available, the efficiency of the engine alone, the efficiency of the transmission alone for a constant speed condition, and the efficiency of the powertrain, were plotted in the coordinates ω_{ICE}, T_{ICE} . As an example, in Figure 5-7 the maps for $v = 10, 35, 60$ km/h are reported.

The maps of Figure 5 are representative of the low speed operating conditions of the vehicle; they show that, passing from Figure 5a to Figure 5c, the optimal line moves to the left, leaning on the maximum torque curve; this behavior is due to the monotonic decrease of the transmission efficiency with increasing engine speed along the iso-power lines (Figure 5b). The transmission for low vehicle speeds, as in this case, works constantly in first gear.

In the intermediate speeds (25 -35 km/h) the gear change occurs and affects the transmission behavior, as shown in Figure 6b. In fact, the best efficiency line of the transmission changes abruptly trajectory because of the synchronous shift between the second and the first gear. This change occurs along the iso-power curve of 125 kW, passing from the optimal engine speed of 1130 to 1540 rpm. The optimum efficiency of the transmission, at the same vehicle speed, takes place in second gear for low power levels, but in first gear if power ratings higher than 125 kW are required. However, variations in transmission efficiency are not sufficient to affect the maximum efficiency line of the entire system (Figure 6c), which is similar to that in Figure 5c.

For high speeds (Figure 7) the second gear is the only possible solution. Unlike the previous case, the efficiency of the transmission shifts the maximum efficiency line significantly towards higher engine speeds.

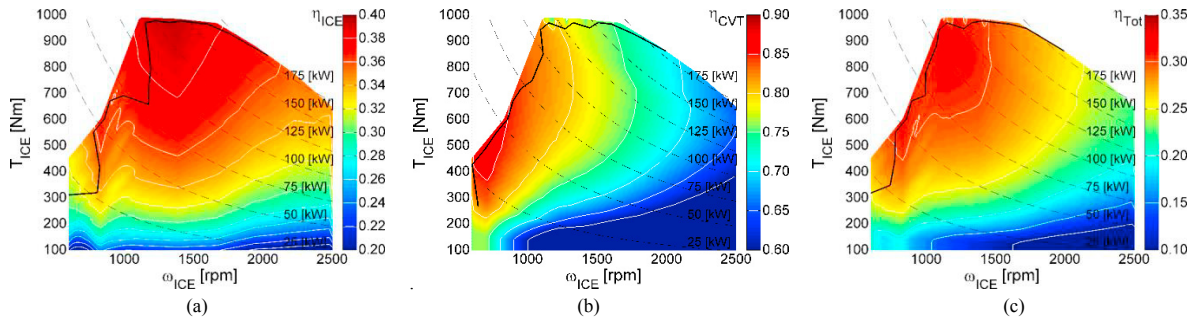


Fig. 5. Best efficiency lines: a) ICE; b) CVT with $v = 10$ km/h; c) Powertrain with $v = 10$ km/h.

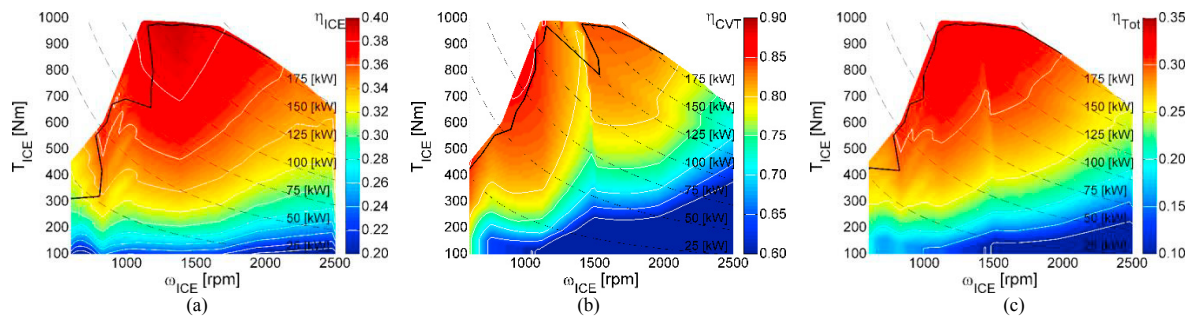


Fig. 6. Best efficiency lines: a) ICE; b) CVT with $v = 25$ km/h; c) Powertrain with $v = 25$ km/h.

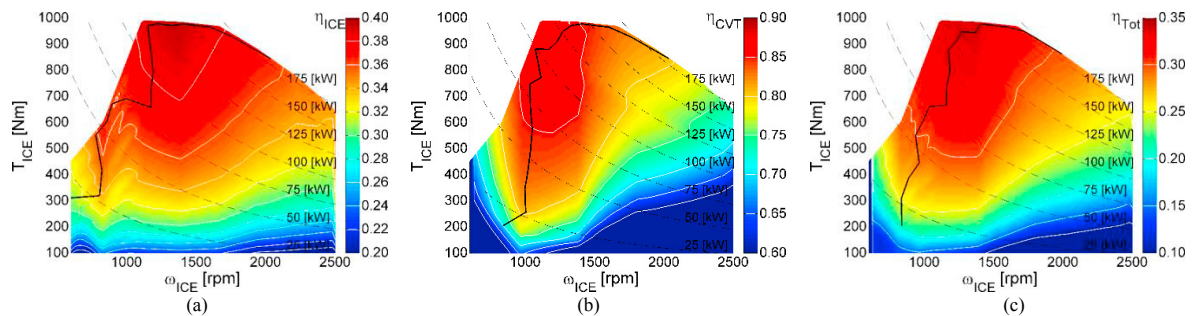


Fig. 7. Best efficiency lines: a) ICE; b) CVT with $v = 60$ km/h; c) Powertrain with $v = 60$ km/h.

4.2. Mission performances

To evaluate the impact of the engine management on the powertrain efficiency, dynamic simulations of the vehicle on mission were carried out. Three different standardized cycles for the characterization of emissions were considered: the New York Bus Cycle, the Manhattan Bus Cycle, and the Composite Urban Emission Drive Cycle (CUED). The first two cycles refer to urban driving condition, while the CUED is divided in four different parts representing congested, residential/minor routes, arterial and highway driving conditions. The main parameters of the selected missions are reported in Table 4.

The simulations were carried out for both the above-mentioned management criteria (optimal engine control OEC, and optimal powertrain control OPC), using the same set-up for the controller implemented with the pilot function. In addition, the adherence of the actual speeds to the mission speeds has been verified for all cases to be comparable between the two control systems.

The simulation results, expressed in terms of fuel consumption, are shown in Table 5. As shown by the table, the OPC criterion, i.e. the optimal management criterion for the entire powertrain, allows an average performance improvement of 2% in the three urban cycle missions (Manhattan Bus, New York Bus, CUED-Congested).

Figure 8 shows the comparison between the operating points of the two control criteria for the Manhattan Bus Cycle mission, which is characterized by low speeds and frequent starts.

Table 4. Mission Details

	Driving Distance	Duration	Idle Time	Max. Speed	Av. Speed	Ave. Speed (w/o stops)	Av. Acceleration (w/o stops)
	km	s	%	km/h	km/h	km/h	m/s ²
Manhattan	3.3	1100	34.9	40.8	12	16.9	0.5
NY	1.0	600	64.4	49.5	5.9	16.7	1.1
CUED -Congested	1.0	322	31.7	36.4	11.1	16.3	5.3
CUED -Minor	4.7	506	1.2	60.7	33.3	33.7	4.4
CUED -Arterial	2.9	435	28	63.3	23.7	33	6.6
CUED -Freeway	5.8	414	5.3	85	50.8	53.7	3.1

Table 5. Fuel consumption

Mission	OEC	OPC	Δ [%]
	kg	kg	
Manhattan	1.293	1.270	- 2.6
New York	0.494	0.481	- 1.8
CUED -Congested	0.408	0.400	-2.0
CUED -Minor	1.375	1.355	-1.4
CUED -Arterial	1.042	1.030	-1.1
CUED -Freeway	1.507	1.479	-1.9

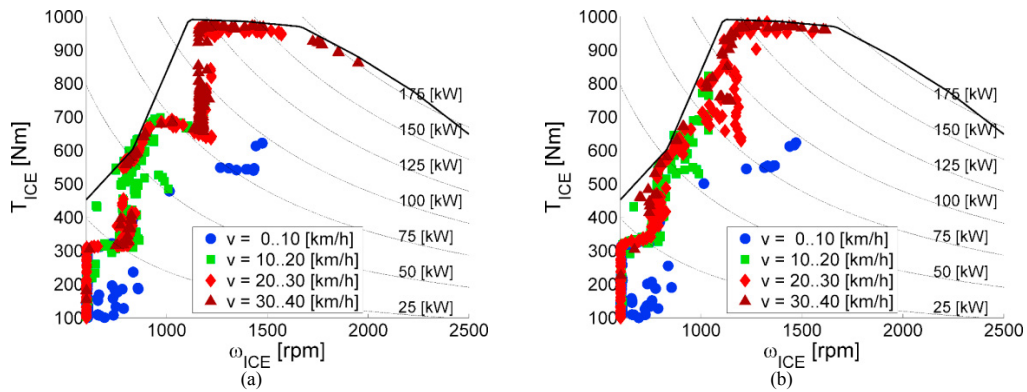


Fig. 8. Actual ICE working condition, Manhattan Bus Cycle: a) OEC; b) OPC.

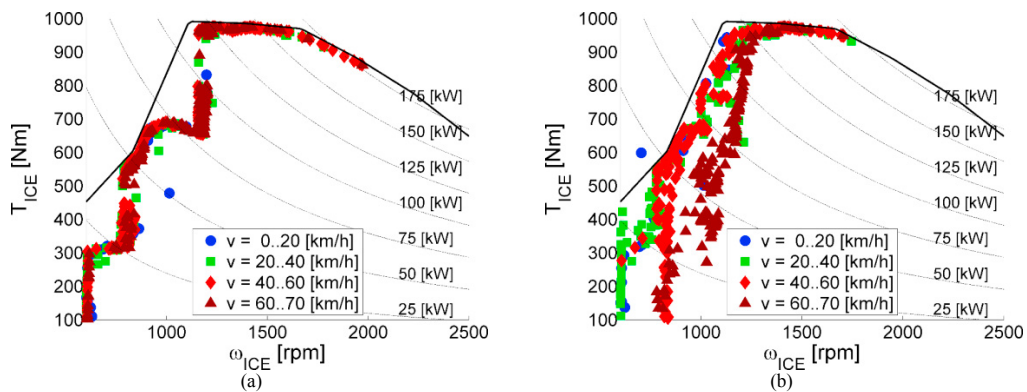


Fig. 9. Actual ICE working condition, CUED-Freeway: a) OEC; b) OPC

The position of the operating points in the map is adherent to the target line for both control criteria. The most significant difference between them occurs in the 75 to 125 kW range, where the second one imposes lower speeds at the same power requirement.

Figure 9 shows the path of the operating points for the CUED-Freeway mission, which is marked by significantly higher speeds. Also in this case, the powertrain optimized control leads to an appreciable advantage (2% reduction in consumption). The differences in behavior of the two control systems are more accentuated with respect to the case of reduced speeds (case of Figure 8).

In particular, the operating points move towards higher engine speeds as the vehicle speed increases, consistently with the behavior of the best efficiency line of Figure 7c.

5. Conclusions

In this paper the management of the engine equipped with continuous hydro-mechanical transmission has been studied.

This problem has been addressed with the aim of providing on-board management rules. The minimum specific fuel consumption line for the whole powertrain has been identified, in analogy with what is usually done for the engine alone. In this way, no complexity has been added to the powertrain control system, but only different minimum lines.

This concept has been applied to the case of an urban bus equipped with a dual-stage hydromechanical transmission. The simulation model of the vehicle was first used to derive the minimum fuel consumption lines for the powertrain, then to simulate the same vehicle using two management criteria: the first one follows the minimum fuel consumption line for the engine alone; the second one follows the lines minimizing the powertrain losses previously calculated.

The result shows that the second criterion guarantees a consumption reduction of about 2%, both in congested urban routes, and in motorway routes.

References

- [1] Jixin Wang, Zhiyu Yang, Shaokang Liu, Qingyang Zhang and Yunwu Han. A comprehensive overview of hybrid construction machinery. *Advances in Mechanical Engineering* 2016, Vol. 8(3) 1–15 2016. DOI: 10.1177/1687814016636809
- [2] Tianliang Lin, Qingfeng Wang, Baozan Hu, Wen Gong. Development of hybrid powered hydraulic construction machinery. *Automation in Construction*. Volume 19, Issue 1, January 2010, Pages 11–19.
- [3] P. Casoli, A. Gambarotta, N. Pompini, L. Riccò (2016) “Hybridization methodology based on DP algorithm for hydraulic mobile machinery — Application to a middle size excavator” *Automation in Construction* Volume 61, January 2016, Pages 42–57. doi:10.1016/j.autcon.2015.09.012.
- [4] Pintore F, Borghi M, Morselli R, Benevelli A, Zardin B, Belluzzi F. Modelling and Simulation of the Hydraulic Circuit of an Agricultural Tractor. *ASME. Fluid Power Systems Technology*, 8th FPNI Ph.D Symposium on Fluid Power():V001T04A004. doi:10.1115/FPNI2014-7848.
- [5] M. Inderelst, S. Losse, S. Sgro, H. Murrenhoff, Energy efficient system layout for work hydraulic of excavators, *The Twelfth Scandinavian International Conference on Fluid Power*, 2011.
- [6] Kress JH. Hydrostatic power splitting transmissions for wheeled vehicles – classification and theory of operation. SAE paper 680549. Warrendale (PA): Society of Automotive Engineers; 196
- [7] Renius KT, Resch R. Continuously variable tractor transmissions, *ASAE Distinguished Lecture Series*, tractor Design No. 29; 2005.
- [8] Casoli P., Vacca A., G., Berta, Meleti S., Vescovini M. (2007) “A numerical model for the simulation of Diesel/CVT power split transmission” SAE paper n. 2007-24-137, SAE-NA ICE2007, 17-20 Settembre, 2007 Capri-Napoli. ISBN: 978-88-900399-3-0. DOI: 10.4271/2007-24-0137
- [9] Blake C, Ivantysynova M, Williams K. Comparison of Operational Characteristics in Power Split Continuously Variable Transmissions. SAE 2006 Commercial Vehicle Engineering Congress & Exhibition, October 2006, *SAE Technical Paper series 2006-01-3468*
- [10] Linares P, Méndez V, Catalán H. Design parameters for continuously variable power-split transmissions using planetaries with 3 active shafts. *J Terramechanics* 2010;47(5):323–35.
- [11] Macor, A., Rossetti, A., 2011. Optimization of hydro-mechanical Power-Split transmissions. *Mech. Mach. Theory* 46, 1901–1919.
- [12] Rossetti A., Macor A., Scamperle M. "Optimization of components and layouts of hydromechanical transmissions" *International Journal of Fluid Power* Volume 18, Issue 2, 4 May 2017, Pages 123-134. DOI: 10.1080/14399776.2017.1296746. Codice Scopus:2-s2.0-85015076287
- [13] Macor, A., Rossetti, A., 2013. Fuel consumption reduction in urban buses by using Power Split transmissions. *Energy Convers. Manage.* 71, 159–171.
- [14] Pffiffer, R., Guzzella, L.R., Onder, C.H., 2003. Fuel-optimal control of CVT powertrains. *Contr. Eng. Pract.* 11, 329–336.
- [15] Bayindir, K.C., Gozukucuk, M.A., Teke, A., 2011. A comprehensive overview of hybrid electric vehicle: powertrain configurations, powertrain control techniques and electronic control units. *Energy Convers. Manage.* 52, 1305–1313.
- [16] Pisu, P., Rizzoni, G., 2007. A comparative study of supervisory control strategies for hybrid electric vehicles. *IEEE Trans. Control Syst. Technol.* 15 (3).
- [17] Shabbir, W., Evangelou, S.A., 2014. Real-time control strategy to maximize hybrid electric vehicle powertrain efficiency. *Appl. Energy* 135, 512–522.
- [18] Montazeri-Gh, M., Mahmoodi-K, M., 2015. Development a new power management strategy for Power Split hybrid electric vehicles. *Transp. Res. Part D* 37, 79–96.
- [19] Wu, B., Lin, C.-C., Filipi, Z., Peng, H., Assanis, D., 2004. Optimal power management for a hydraulic hybrid delivery truck. *J. Veh. Syst. Dynam.* 42 (1), 23–40.
- [20] Stelson, K.A., Meyer, J.J., Hency, B., 2008. Optimization of a passenger hydraulic hybrid vehicle to improve fuel economy. In: *Proceedings of the 7th JFPS International Symposium on Fluid Power*, Toyama 2008 September 15–18, 2008.
- [21] Hiremath, S.S., Ramakrishnan, R., Singaperumal, M., 2013. Optimization of process parameters in series hydraulic hybrid system through multi-objective function. In: *The 13th Scandinavian International Conference on Fluid Power*, SICFP2013, June 3–5, 2013, Linköping, Sweden.
- [22] AMESim, 2016. Copyright 1996–2016, LMS Imagine SA.
- [23] Kim J, Kang J, Kim Y, Kim T, Min B, Kim H. Design of Power Split transmission: design of dual mode Power-Split transmission. *International Journal of Automotive Technology*, vol. 11, no. 4, pp. 565–571 (2010).